Synthesis and Characterization of Superconducting β-Mo_2N Crystalline Phase on a Si Substrate: An Application of Pulsed Laser Deposition to Nitride Chemistry

Kei Inumaru,* Kazuya Baba, and Shoji Yamanaka

Department of Applied Chemistry, Faculty of Engineering, Hiroshima University, Higashi-Hiroshima 739-8527, Japan

Received April 2, 2005. Revised Manuscript Received July 26, 2005

Molybdenum nitride β-Mo_2N was synthesized on Si substrates by pulsed laser deposition of molybdenum metal under nitrogen radical irradiation. X-ray diffraction studies using a multiaxes diffractometer revealed that the crystal phase had a tetragonal structure uniaxially oriented with (100) planes parallel to the substrate surface. The composition was determined to be $Mo_2N_{0.85}$ by calibrated X-ray photoelectron spectroscopy. These results demonstrated that the well-crystallized tetragonal-phase β-Mo_2N was synthesized by deposition, rather than a cubic γ-phase with randomly distributed nitrogen vacancies. The nitride β-Mo_2N was superconducting below 5.2 K.

Introduction

The chemistry of metal nitrides is less explored compared with metal oxide chemistry. Chemistry of nitrides was developed in the 1930s−1970s by scientists including Juza. Recently, increasing interest on chemical and physical properties of nitrides has accelerated studies on binary and ternary nitrides.[1−3] Recent studies report the synthesis of novel ternary nitrides containing alkaline-earth and transition metal elements,[4,5] the unique electronic structure of alkaline-earth nitrides,[6] Li intercalation,[7,8] large crystal growth of GaN using Na flux,[9] and novel layered Sr nitrides.[10] For transition metal binary nitrides, a wide variety of physical properties has been reported.[11−34] For example, 3d transition metal nitrides showed antiferromagnetism (MnN,[11,12] CrN,[13,14] FeN[16]), Pauli paramagnetism[17] (CoN), and superconductivity[34] (TiN, VN). Discovery of the electron-doped layered

* To whom correspondence should be addressed. Phone: +81-82-424-7741. Fax: +81-82-424-5494. E-mail: inumaru@hiroshima-u.ac.jp.

(1) (a) Simon, A. *Coord. Chem. Rev.* **1997**, *163*, 253. (b) Simon, A. *Angew. Chem., Int. Ed. Eng.* **1997**, *36*, 1789.
(2) Niewa, R.; DiSalvo, F. J. *Chem. Mater.* **1998**, *10*, 2733.
(3) (a) Gregory, D. H. *Coord. Chem. Rev.* **2001**, *215*, 301. (b) Gregory, D. H. *J. Chem. Soc., Dalton Trans*. **1999**, 259.
(4) (a) Bailey, M. S.; Obrovac, M. N.; Baillet, E.; Reynolds, T. K.; Zax, D. B.; DiSalvo, F. J. *Inorg. Chem.* **2003**, *42* 5572. (b) Bailey, M. S.; McGuire, M. A.; DiSalvo, F. J. *Z. Anorg. Allg. Chem.* **2004**, *630*, 2177.
(5) Farault, G.; Gautier, W.; Baker, C. F.; Bowman, A.; Gregory, D. H. *Chem. Mater*. **2003**, *15*, 3922.
(6) Steinbrenner, U.; Simon, A. *Z. Anorg. Allg. Chem* **1998**, *624*, 228.
(7) Gulo, F.; Simon, A.; Kohler, J.; Kremer, R. K. *Angew. Chem., Int. Ed*. **2004**, *43*, 2032.
(8) Gordon, A. G.; Smith, R. I.; Wilson, C.; Stoeva, Z.; Gregory, D. H. *Chem. Commun.* **2004**, 2812.
(9) Aoki, M.; Yamane, H.; Shimada, M.; Iwata, H.; DiSalvo, F. J. *J. Cryst. Growth* **2004**, *266*, 461.
(10) (a) Prots, Y.; Auffermann, G.; Tovar, M.; Kniep, R. *Angew. Chem., Int. Ed*. **2002**, *41*, 2288. (b) Auffermann, G.; Prots, Y.; Kniep, R. *Angew. Chem., Int. Ed.* **2001**, *40*, 547.
(11) (a) Suzuki, K.; Kaneko, T.; Yoshida, H.; Obi, Y.; Fujimori, H.; Morita, H. *J. Alloys Compd.* **2000**, *306*, 66. (b) Suzuki, K.; Suzuki, T.; Fujiwara, Y.; Kaneko, T.; Yoshida, H.; Obi, Y.; Tomiyoshi, S. *J. Alloys Compd.* **2003**, *360*, 34.
(12) (a) Yang, H. Q.; Al-Brithen, H.; Trifan, E.; Ingram, D. C.; Smith, A. R. *J. Appl. Phys.* **2002**, *91*, 1053. (b) Yang, H. Q.; Al-Brithen, H.; Smith, A. R.; Borchers, J. A.; Cappelletti, R. L.; Vaudin, M. D. *Appl. Phys. Lett.* **2001**, *78*, 3860.
(13) Suzuki, K.; Kaneko, T.; Yoshida, H.; Obi, Y.; Fujimori, H. *J. Alloys Compd.* **1998**, *280*, 294.
(14) (a) Filippetti, A.; Hill, N. A. *Phys. Rev. Lett.* **2000**, *85*, 5166. (b) Filippetti, A.; Pickett, W. E.; Klein, B. M. *Phys. Rev. B* **1999**, *59*, 7043.
(15) Herle, P. S.; Hedge, M. S.; Vasathacharya, N. Y.; Philip, S. *J. Solid State Chem.* **1997**, *134*, 120.
(16) Hinomura, T.; Nasu, S. *Physica B* **1997**, *237−238*, 557.
(17) Suzuki, K.; Kaneko, T.; Yoshida, H.; Morita, H.; Fujimori, H. *J. Alloys Compd.* **1995**, *224*, 232.
(18) Takeuchi, N. *Phys. Rev. B* **2002**, *66*, 153405.
(19) Smith, A. R.; Al-Brithen, H.; Ingram, D. C.; Gall, D. *J. Appl. Phys.* **2001**, *90*, 1809.
(20) Frazier, R. M.; Stapleton, J.; Thaler, G. T.; Abernathy, C. R.; Pearton, S. J.; Rairigh, R.; Kelly, J.; Hebard, A. F.; Nakarmi, M. L.; Nam, K. B.; Lin, J. Y.; Jiang, H. X.; Zavada, J. M.; Wilson, R. G. *J. Appl. Phys.* **2003**, *94*, 1592.
(21) Pearton, S. J.; Park, Y. D.; Abernathy, C. R.; Overberg, M. E.; Thaler, G. T.; Kim, J.; Ren, F. *J. Electron. Mater.* **2003**, *32*, 288.
(22) Lee, J. S.; Lim, J. D.; Khim, Z. G.; Park, Y. D.; Pearton, S. J.; Chu, S. *J. Appl. Phys.* **2003**, *93*, 4512.
(23) (a) Inumaru, K.; Ohara, T.; Yamanaka, S. *Appl. Surf. Sci.* **2000**, *158*, 375. (b) Inumaru, K.; Ohara, T.; Tanaka, K.; Yamanaka, S. *Appl. Surface Sci.* **2004**, *235*, 460.
(24) Inumaru, K.; Okamoto, H.; Yamanaka, S. *J. Cryst. Growth* **2002**, *237−239*, 2050.
(25) Inumaru, K.; Sakamoto, K.; Okamoto, H.; Yamanaka, S. *Physica B* **2003**, *328*, 123.
(26) Sakamoto, K.; Inumaru, K.; Yamanaka, S. *Appl. Surf. Sci.* **2002**, *199*, 303.
(27) Inumaru, K.; Kuroda, Y.; Sakamoto, K.; Murashima, M.; Yamanaka, S. *J. Alloys Compd.* **2004**, 372, L1.
(28) Johansson, B. O.; Sundgren, J. E.; Greene, J. E.; Rockett, A.; Barnett, A. *J. Vac. Sci. Technol., A* **1985**, *3*, 303.
(29) Hirashita, N.; Greene, J. E.; Helmersson, U.; Birch, J.; Sundgren, J.-E. *J. Appl. Phys.* **1991**, *70*, 4963.
(30) Kumar, A.; Chan, H. L.; Ekanayake, U.; Wierzbicki, A.; Dahotre, N. B. *J. Mater. Eng. Perform.* **1997**, *6*, 577.
(31) (a) Timm, R.; Willmott, P. R.; Huber, J. R. *Appl. Phys. Lett.* **1997**, *71*, 1966. (b) Willmott, P. R.; Timm, R.; Huber, J. R. *Appl. Surf. Sci.* **1998**, *129*, 105.
(32) Lee, M. B.; Kawasaki, M.; Yoshimoto, M.; Kumagai, M.; Koinuma, H. *Jpn. J. Appl. Phys.* **1994**, *33*, 6308.
(33) Mancera, L.; Rodriguez, J. A.; Takeuchi, N. *J. Phys. Condens. Matter* **2003**, *15*, 2625.
(34) George, H. F.; John, H. K. *Phys. Rev.* **1954**, *93*, 1004.

10.1021/cm050708i CCC: $30.25
Published on Web 10/29/2005

hafnium nitride superconductor β-HfNCl with a transition temperature (T_c) of as high as 25.5 K[35] stimulated interest in the superconductivity of metal nitrides.

Molybdenum nitrides have attracted attention as superconducting materials. Molybdenum forms several crystalline nitrides, including γ-Mo_2N (cubic), β-Mo_2N (tetragonal), and hexagonal δ-MoN.[36] It was reported that hexagonal MoN was crystallized in a slightly distorted NiAs type structure under 6 GPa,[37,38] and the resulting phase showed superconductivity with $T_c \sim 12$ K.[37,39] Since a theoretical study predicted that MoN with cubic NaCl type structure (so-called B1−MoN) would have T_c as high as 39 K,[40] many researchers have attempted to synthesize B1−MoN. However, there is still no report on well-crystallized B1−MoN having such a high T_c. γ-Mo_2N is also known as a superconductor ($T_c = 5$ K).[39] Mo_2N crystallizes in two crystal forms: γ-Mo_2N and β-Mo_2N.[41] γ-Mo_2N is a face centered cubic phase with randomly distributed nitrogen in octahedral sites. β-Mo_2N is a tetragonal phase and is believed to have ordered nitrogen sites, with a doubled *c*-parameter compared to γ-Mo_2N.[37,41] Many studies have reported the synthesis of γ-Mo_2N as a hard-coat material.[42−44] On the other hand, few studies reported the synthesis and characterization of the well-crystallized β-Mo_2N. This is probably because β-Mo_2N readily transforms to γ-Mo_2N at high temperatures.[37,41]

Thin films and superlattices of transition metal nitrides also attracted much attention.[11−13,17−33,45] We have reported layer-by-layer growth of TiN and CrN−TiN multilayers,[23] epitaxial CrN growth on Si,[24] the first synthesis of oriented Sr_2N layered nitride film,[27] and the synthesis of novel nitride solid solution $Ni_xTi_{1-x}N_y$.[26] The thin film studies in the literature and our studies highlight the use of thin film deposition as a versatile synthetic technique for nitrides. An advantage of thin film techniques is that ultrahigh-vacuum chambers avoid oxygen contamination under the synthetic processes. However, a disadvantage is that crystalline phases in thin films tend to show preferred orientation, and it is rather difficult to analyze and determine crystal parameters because they give only a few diffraction peaks detectable by conventional X-ray diffraction measurements.

Here we report the synthesis of well-crystallized β-Mo_2N as thin films by pulsed laser deposition (PLD). Analysis by X-ray diffraction measurements with multiaxes sample movements enabled the determination and refinement of crystal cell parameters even for the oriented phase on the substrates. Superconductivity of β-Mo_2N was also explicitly reported here, for the first time.

Table 1. Conditions for Molybdenum Nitride Deposition[a]

sample	T_s/K	r_{av}/(nm h^{-1})	t_f/nm
sample A	973	54	108
sample B	973	1.3	8.7
sample C	673	42	95

[a] T_s, substrate temperature; r_{av}, average deposition rate; t_f, film thickness.

Experimental Section

Materials. A metallic Mo disk (99.9%, 1 cm in diameter, 0.5 cm in thickness) was purchased from Niraco Co. (Tokyo) and was used as the target for PLD after washing with ethanol. $MoCl_5$ was obtained from Aldrich and was used without further treatment. Si (001) wafers (ShinEtsu Chemical Co.) were used as substrates. Prior to use, the wafers were washed with acetone ultrasonically. N_2 gas (99.9999%) was obtained from Nippon Sanso Co. and was used to generate nitrogen radicals.

Synthesis of Mo_2N Powder Samples. $MoCl_5$ powder (ca. 0.2 g) contained in an Al_2O_3 boat was placed into a quartz tube furnace. Under a flow of mixed gas of N_2 and H_2 (1:4 (v/v); total flow rate, 200 cm^3/min), the material was heated at the rate of 10 K/min up to 923 K and nitrided at 923 K for 3 h. Oxygen impurities in the mixed gas were removed by passing through a de-oxygenation column.[46] This column consists of two parts: The gas flows through a 5 wt % Pt/γ-Al_2O_3 catalyst bed and then flows through a molecular sieve 13X bed. O_2 contamination reacts over Pt/γ-Al_2O_3 with H_2 to form H_2O, which is removed by the molecular sieve bed. Powder X-ray diffraction analysis confirmed that the product was γ-Mo_2N. The nitrogen content of the γ-Mo_2N sample was determined with an elemental analyzer (PerkinElmer 2400II). The sample was heated to 2000 K in pure oxygen, and the evolved nitrogen oxides were analyzed. The composition of the γ-Mo_2N powder sample prepared in this study was $Mo_2N_{0.84}$.

Synthesis of Molybdenum Nitride on Si Substrates. The PLD system was equipped with a KrF excimer laser (COMPex102, Lambda Physics, Goettingen, Germany) and an RF-plasma radical source (model RF4.5, SVTA, Eden Prairie, MN). The residual pressure of the chamber was less than 10^{-8} Torr. The metallic Mo disk (99.9%) was used as the target. Si substrates were cleaned in acetone before their introduction into the vacuum chamber. Nitride films were deposited under irradiation of nitrogen radicals (RF power, 350 W; N_2 feed, 0.3 cm^3(STP)/min). The pulse repetition rate was 20 Hz. The deposition rate was controlled by changing the power of the laser pulses (80−300 mJ). Deposition conditions for samples denoted by A−C are listed in Table 1. Thickness of the thin films was determined using an atomic force microscope (AFM).

X-ray Diffraction Analysis of the Oriented Crystalline Nitride Phase. The crystal structure of the nitride phase on substrates was characterized by X-ray diffraction using two diffractometers. Simple conventional $\omega - 2\theta$ scans were performed with an M18FHX diffractometer (MacScience, Tokyo) using Cu Kα radiation. The measurements with this apparatus detected diffraction peaks from crystal planes parallel to the substrate surface. γ-Mo_2N powder was also measured with this diffractometer. For cell parameter determination of the crystal phase, a diffractometer with a multiaxes sample stage (XPert MRD, Philips, The Netherlands) was used to measure crystal planes not parallel to the surface. The incident beam was a Cu Kα parallel beam from an X-ray mirror with a crossed

(35) Yamanaka, S.; Hotehama, K.; Kawaji, H. *Nature* **1998**, *392*, 580.
(36) Jehn, H.; Ettmayer, P. *J. Less-Common Met.* **1978**, *58*, 85.
(37) Bull, C. L.; McMillan, P. F.; Soignard, E.; Leinenweber, K. *J. Solid State Chem.* **2004**, *177*, 1488.
(38) Bezinge, A.; Yvon, K.; Muller, J. *Solid State Commun.* **1987**, *63*, 141.
(39) Matthias, B. T.; Hulm, J. K. *Phys. Rev.* **1952**, *87*, 799.
(40) (a) Papaconstantopoulos, D. A.; Pickett, W. E.; Klein, B. M.; Boyer, L. L. *Nature* **1984**, *308*, 494. (b) Papaconstantopoulos, D. A.; Pickett, W. E.; Klein, B. M.; Boyer, L. L. *Phys. Rev. B* **1985**, *31*, 752.
(41) Ettmayer, P. *Montash. Chem.* **1970**, *101*, 127.
(42) Wang, Y. M.; Lin, R. Y. *Mater. Sci. Eng., B* **2004**, *112*, 42.
(43) Anitha, V. P.; Major, S.; Chandrashekharam, D.; Bhatnager, M. *Surf. Coat. Technol.* **1996**, *79*, 50.
(44) Bereznai, M.; Tóth, Z.; Caricato, A. P.; Fernández, M.; Luches, A.; Majni, G.; Mengucci, P.; Nagy, P. M.; Juhász, A.; Nánai, L. *Thin Solid Films* **2005**, *473*, 16.
(45) Willmott, P. R. *Prog. Surf. Sci.* **2004**, *76*, 163.
(46) Zhu, L.; Ohashi, M.; Yamanaka, S. *Mater. Res. Bull.* **2002**, *37*, 475.

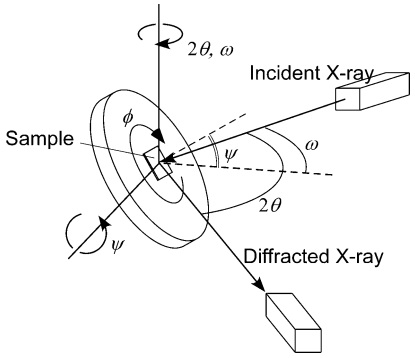

Figure 1. Schematic illustration of multiaxes sample movement of the X-ray diffractometer.

slit (0.5 mm width and 5 mm height). The detector was equipped with a parallel-plate collimator and graphite monochromator (resolution, 0.27°). Figure 1 shows a schematic illustration of the multiaxes system. We fixed ϕ angle and used three axes for the measurement, i.e., ω, ψ, and θ: For a certain diffraction (hkl), ψ, ω, and 2θ were calculated by using assumed cell parameters. Axes were moved to the angles and $\omega - 2\theta$ scans were performed at the calculated angle of ψ (not zero).

Other Characterizations. Magnetic properties were measured with an MPMS-5S magnetometer (Quantum Design, San Diego, CA). The angle between the magnetic field and the substrate was ca. 45°. The electric resistance of sample A was measured by a four-probe method. The temperature of the sample was controlled in the range of 2−15 K with the MPMS-5S. AFM images were taken with a Nanoscope D-3100 (Digital Instrument) operated in tapping mode. Compositions of the thin films were determined by X-ray photoelectron spectroscopy (ESCA850, Shimadzu, Japan): Mo 3d, Mo $3p_{3/2}$, and N $1s_{1/2}$ spectra were measured for γ-Mo_2N powder sample, whose composition was determined by chemical analysis in this study. Prior to measurement of XPS data, the sample surface was cleaned up by in-situ Ar sputtering. Spectra were separated by a curve fitting, and the intensities of Mo $3p_{3/2}$ and N $1s_{1/2}$ were used to calibrate the relative sensitivity factors of the spectrometer for the two signals. Mo $3p_{3/2}$ and N $1s_{1/2}$ spectra of thin films were separated by the same procedures, and compositions were calculated using the calibrated sensitivity factors.

Results

Conventional X-ray Diffraction Analysis. Figure 2 shows X-ray diffraction patterns (conventional $\omega - 2\theta$ scan) of molybdenum nitride on Si substrate synthesized under different conditions. For sample A (Figure 2a), two sharp peaks ($d = 0.2099$ and 0.1050 nm) were observed, indicating that a well-crystallized phase was formed, and the crystal phase had some preferred orientations on the substrate. In Figure 2, some calculated diffraction patterns are also shown for molybdenum nitride phases reported in the literature (Figure 2b−2d). Comparison of these patterns suggested that the crystalline phase was β-Mo_2N or γ-Mo_2N, and the observed peaks could be indexed as 200 and 400. Table 2 compares the d values obtained for sample A and those for the molybdenum nitride phases reported in the literature. β-Mo_2N is a tetragonal phase, and γ-Mo_2N is a cubic phase. The d values for the thin film (0.2099 and 0.1050 nm) were closer to the calculated β-Mo_2N (200) and (400) (0.2094 and 0.1047 nm) rather than to γ-Mo_2N (200) and (400) (d = 0.2082 and 0.1031 nm), indicating the β-Mo_2N as the most probable candidate. As shown in the inset of Figure 2, the X-ray diffraction peak position is close to the β-Mo_2N 204 position (43.16°) and is clearly distinguishable from the γ-Mo_2N 202 position (43.425°). Concerning this point, further analysis was performed as will be described in a later section.

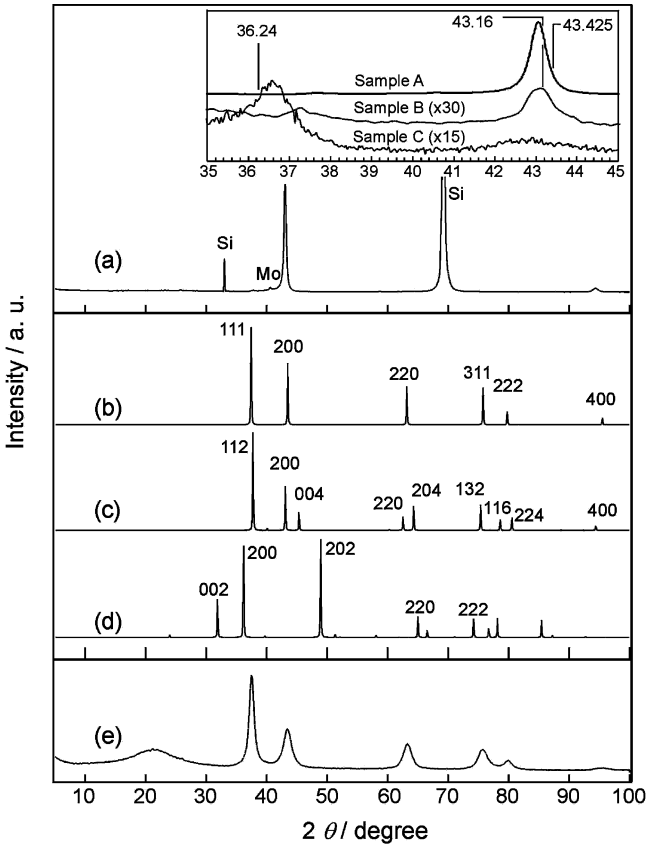

Figure 2. X-ray diffraction patterns of molybdenum nitride deposited on Si substrates and γ-Mo_2N powder prepared in this study. (a) Sample A. Patterns b−d represent calculated diffraction patterns for γ-Mo_2N, β-Mo_2N, and δ-MoN, respectively. Panel e shows diffraction patterns for γ-Mo_2N powder prepared in this study. The inset shows magnified patterns for samples A−C. In the inset, several calculated positions were indicated for γ-Mo_2N 202 (43.425°), β-Mo_2N 204 (43.16°), and δ-MoN 200 (36.24°).

Table 2. Comparison of X-ray Diffraction *d* Spacing for Molybdenum Nitride Films

	d-spacing/nm (2θ)		Cell parameters/nm	
sample	$d_{(200)}$	$d_{(400)}$	A	c
sample A	0.2099 (43.05°)	0.1050 (94.40°)	0.41991(8)[a]	0.7996(7)[a]
sample B	0.2096 (43.12°)	0.105 (94.4°)		
sample C	0.2114 (42.73°)	nd		
γ-Mo_2N (powder)	0.2082 (43.43°)	0.1040 (95.62°)	0.4155(3)	
γ-Mo_2N[b]	0.2082	0.1041	0.4165	
β-Mo_2N[c]	0.2094	0.1047	0.4188	0.8048

[a] Refined on the basis of multiaxes X-ray diffraction data. See text. [b] ICSD 76281; PDF card 251366. [c] PDF card 251368.

A significant decrease of the average deposition rate (r_{av}) from 54 to 1.3 nm/h (sample B) did not affect X-ray diffraction peak positions (the inset of Figure 2). Sample C synthesized at a lower temperature (T_s = 673 K) gave a broad X-ray diffraction peak slightly at a lower angle than samples A and B, suggesting formation of a poorly crystallized nitrogen-rich film. Another weak and broad peak was observed at a lower angle, of which the position was at a slightly higher angle than calculated position for δ-MoN 200

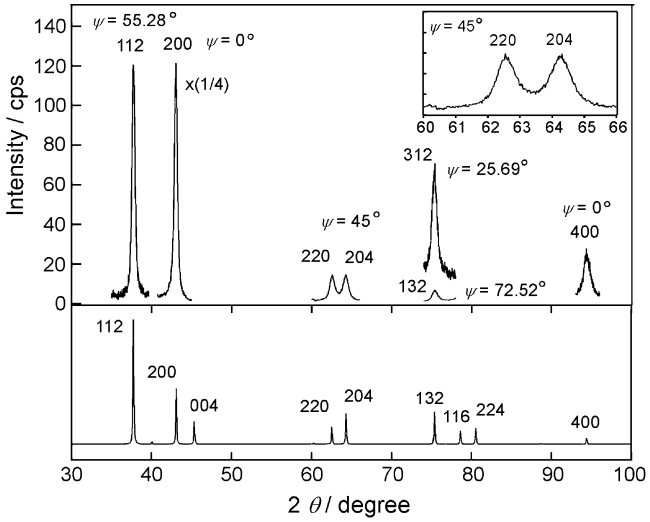

Figure 3. X-ray diffraction patterns of the molybdenum nitride on Si (sample A) measured at various Ψ angles. Calculated powder pattern for β-Mo_2N is shown for comparison in the bottom panel. The inset shows a magnified pattern at $\Psi = 45°$.

($2\theta = 36.24°$). A possibility is that nitrogen-deficient δ-MoN was partly formed in sample C. Hereafter, only sample A was used for further characterization.

Figure 2e shows a diffraction pattern for powder γ-Mo_2N prepared in this study. The pattern coincided well with the calculated pattern (Figure 2b). Cell parameters estimated from the observed pattern are also listed in Table 2. Cell parameters coincided well with those reported in the literature.

Since X-ray diffraction patterns (Figure 2a) indicated a preferred orientation of the crystal phase in the film, a rocking curve of sample A was measured for diffraction peak at ca. 43.05°. The curve was relatively broad, and its width at half-maximum was 11.1°, indicating a moderately ordered orientation of the crystal phase. The substrate was a Si wafer and its surface was covered by amorphous silicon oxide layer. Thus, it was unlikely that the crystal phase had strong interactions with the Si crystal wafer, being consistent with the moderate orientation of the crystal phase.

X-ray Diffraction Measurements for Crystal Planes Not Parallel to the Substrate Surface. Because the molybdenum nitride in the film had a preferred orientation, conventional X-ray diffraction measurements (simple $\omega - 2\theta$ scans) gave only limited diffractions. To obtain more information on the lattice constants, diffraction peaks from crystal planes that were not parallel to the substrate surface were measured using the diffractometer equipped with a multiaxes sample stage. The inset in Figure 3 shows diffraction patterns that were measured at a ψ angle of 45°. Two peaks were clearly observed, and their positions coincided well with those of β-Mo_2N 220 and 204 diffractions. Considering the crystal structure of Si substrate (cubic, F-type lattice, $a = 0.543$ nm), it is evident that these peaks are not due to the Si substrate. The existence of the 204 peak excluded the possibility of the cubic phase γ-Mo_2N. Thus, the β-Mo_2N lattice (with c axis parallel to the substrate surface) was assumed for ψ angle calculations of many diffractions, and $\omega - 2\theta$ scans were performed for each diffraction at the calculated ψ. In Figure 3, the results are displayed on a common axis of 2θ for comparison with the calculated X-ray diffraction patterns of β-Mo_2N. The peak positions coincided well with the peaks in the calculated patterns.

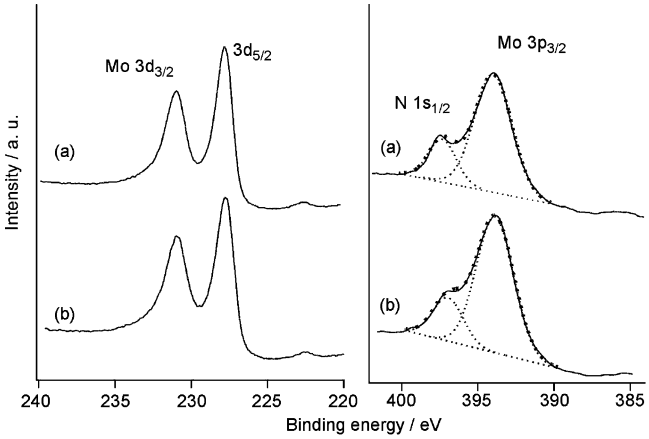

Figure 4. X-ray photoelectron spectra for molybdenum nitride thin film sample A (a) and the powder γ-Mo_2N sample (b).

Table 3. Comparison of X-ray Photoelectron Spectra Binding Energies

	binding energy[a]/ eV			
sample	Mo $3d_{3/2}$	Mo $3d_{5/2}$	Mo $3p_{3/2}$	N $1s_{1/2}$
sample A (β-Mo_2N)	231.0	227.8	393.9	397.5
γ-Mo_2N (powder)	230.9	227.7	393.8	397.1
Mo (metal)[b]		227.85		
Mo_2C[b]		227.8		
MoB_2[b]		227.9		
MoO_3[b]		232.8		
CrN[b]				396.8
Si_3N_4[b]				397.7
BN[b]				398.1

[a] Calibrated by using the $C1s_{1/2}$ signal (284.5 eV). [b] Reference 51.

By using the peak positions in Figure 3, it was possible to refine the lattice constants. When an orthorhombic phase was assumed, a least-squares refinement gave lattice constants of $a = 0.42001(6)$, $b = 0.4196(1)$, and $c = 0.7997(4)$ nm. The a and b values were regarded to be identical when experimental error was taken into account. Therefore, the phase was tetragonal, and cell parameters were refined to be $a = 0.41991(8)$ and $c = 0.7996(7)$ nm. These values are very close to those reported for β-Mo_2N. These results demonstrated that the crystal phase on the substrate was β-Mo_2N with a moderate orientation in which the c axis is parallel to the Si substrate surface.

Characterization by X-ray Photoelectron Spectroscopy and Atomic Force Microscope. Figure 4 represents Mo 3d and N 1s X-ray photoelectron spectra of the thin film. Prior to measurements, surface contamination was removed by in situ Ar sputtering. Both Mo 3d and N 1s peaks were clearly observed. The position of Mo $3p_{3/2}$ peak was close to that of N 1s peak, and the tail of Mo peak overlapped the N 1s peak.

Table 3 compares binding energies of Mo 3d and N 1s peaks for the thin film with those of Mo-containing compounds reported in the literature. The position of Mo $3d_{5/2}$ for the thin film (227.8 eV) was located close to Mo_2C and Mo metal (227.9 eV). The N 1s signal was close to that of the covalent nitride Si_3N_4 rather than that of the transition metal nitride CrN. These results showed that bonds between

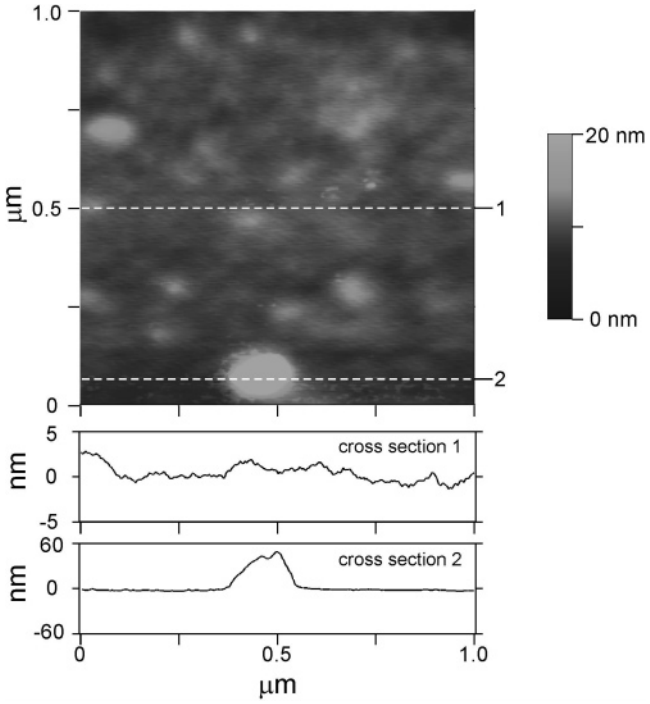

Figure 5. Atomic force microscope image of molybdenum nitride thin film (sample A). Cross sections correspond to dashed lines indicated in the image.

Mo and N were covalent rather than ionic. Figure 4 shows spectra for a bulk γ-Mo_2N powder prepared in this study. The peak positions of Mo were identical to those for the thin film. The N $1s_{1/2}$ peak of the powder γ-Mo_2N had slightly smaller binding energy (by 0.3 eV) with unknown reasons.

Composition of the thin film was determined from the X-ray photoelectron spectra. Peaks of N 1s and Mo $3p_{2/3}$ were separated and their peak area ratio was compared to that for the bulk γ-Mo_2N. Curve fitting for N $1s_{1/2}$–Mo $2p_{3/2}$ separation gave good fitting, as shown in Figure 4. Since the nitrogen content in the bulk γ-Mo_2N was determined by elemental analysis, the sample could be used for calibration of the X-ray photoelectron spectrometer. Relative sensitivity factor for Mo $2p_{3/2}$ and N $1s_{1/2}$ signals were determined experimentally for the spectrometer. Thus, the composition of the molybdenum nitride on Si was determined to be $Mo_2N_{0.85}$.

Figure 5 shows a surface image of sample A observed by AFM. As shown in cross section 1, the surface roughness of the thin film was as small as ca. 3 nm through a horizontal distance of 1 μm, indicating that, during the deposition, molybdenum was properly vaporized by laser ablation to grow flat film. At the bottom of the image, a particle (diameter, ca. 200 nm; height, ca. 50 nm) was observed. The particle observed here might be produced from a droplet that is produced when laser pulses ablated the surface of Mo disk. According to AFM observations, the number of "droplets" on the surface was less than 1 particle/μm^2. It is likely that the very weak peak of Mo observed in the X-ray diffraction pattern (Figure 2a) is due to the droplets. It was possible to calculate Mo crystal thickness from the full width at half-maximum (fwhm) of the X-ray diffraction peak using Sherrer's equation ($D = 0.9\,\lambda/B\cos\theta$, where D is crystal thickness, B is the fwhm, and λ is the wavelength of X-ray). The equation gave Mo crystal thickness of 36 nm. Surface of Mo particles may be nitrided by nitrogen radical irradiation, and possibly the core of the particle is Mo metal. The part of relatively smooth thin film consists of the well-crystallized β-Mo_2N.

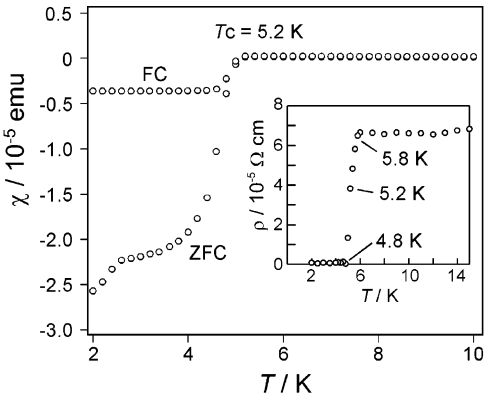

Figure 6. Temperature dependence of magnetic susceptibility of molybdenum nitride thin film (sample A, 0.13 cm^2). The applied field was 19.6 Oe. The inset shows the electric resistance of sample A as a function of temperature.

Magnetic Susceptibility and Electric Resistance Measurements of the Thin Film. Figure 6 shows the temperature dependence of magnetic susceptibility of the molybdenum nitride on Si substrate. Strong diamagnetism demonstrated that the nitride phase was superconducting. The curve for zero-field cooling indicated that the major part of the sample had a transition temperature at 5.2 K. The apparent superconducting fraction of the sample ($-4\pi\chi/V$, where χ is the magnetic susceptibility and V is the sample volume in cm^3; sample dimension, ca. 0.25 × 0.5 cm^2; thickness, 108 nm) was calculated to be 230. This large diamagnetic response is due to local field enhancement arising from the geometric demagnetization factor for a thin film:[47] A simple estimation shows that this sample should have large platelike superconducting domains with diameter 460 times larger than the film thickness. Therefore, this phenomenon cannot be arisen from a minor phase dispersed in the sample. Temperature dependence of the electric resistance of the film was shown in the inset of Figure 6. The T_c (onset) was 5.8 K, and the resistance became zero at 4.8 K, being consistent with the results of the magnetic measurement. It is unlikely that the zero-resistance was attained by a minor superconducting phase dispersed in the sample. These results strongly support that the superconductivity is due to the main phase in the sample, β-Mo_2N.

Discussion

X-ray diffraction and X-ray photoelectron spectroscopy results demonstrated that the crystal phase formed on the substrate was β-Mo_2N. For Mo_2N, two crystal forms were previously reported in the literature: γ-Mo_2N and β-Mo_2N. Figure 7 represents crystal structures of the two phases. γ-Mo_2N is a cubic phase. A face centered cubic ($Fm\bar{3}m$) structure with disordered nitrogen sites was reported.[41,48] On

(47) Thompson, D. J.; Minhaj, M. S. M.; Wenger L. E.; Chen, J. T. *Phys. Rev. Lett.* **1995**, *75*, 529.

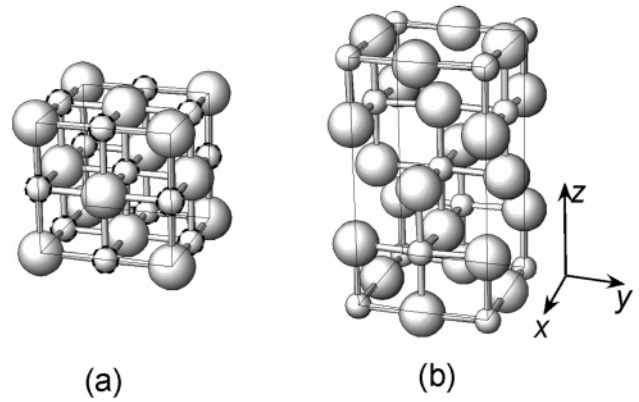

Figure 7. Crystal structure of molybdenum nitrides: (a) γ-Mo_2N; (b) β-Mo_2N. Large and small spheres represent Mo and N atoms, respectively. Nitrogen sites drawn with dashed lines in a indicate partially occupied sites.

the other hand, the N sites in β-Mo_2N were thought to be located in an ordered manner as shown in Figure 7,[41] and the lattice shrinks slightly along the *c* axis compared with γ-Mo_2N.

X-ray diffraction results demonstrated that the β-Mo_2N tetragonal cell ($a = 0.41991(8)$, $c = 0.7996(7)$ nm) was preferentially oriented with the (100) plane parallel to the substrate surface. The refined cell parameters were precisely coincided with those of β-Mo_2N. It is unlikely that the nonstoichiometry caused the contraction only along the *c* axis to make cell parameters fortuitously coincide with the values.

Since the substrate surface was covered by an amorphous oxide layer before deposition of the nitride, it was unlikely that the orientation of the nitride crystal phase was governed by epitaxy. The orientation was probably due to the anisotropic growth rate of crystal and/or different surface energies depending on the crystal planes.

Although β-Mo_2N was reported at an early date, there are limited descriptions of synthesis of well-crystallized β-Mo_2N in the literature. This is probably because β-Mo_2N transforms readily to the cubic phase γ-Mo_2N at 673−1113 K (with the transition temperature depending on nitrogen content).[36,41] Recently, a large number of studies reported on the preparation of molybdenum nitride film. Most studies reported the formation of γ-Mo_2N as crystal phase in the films.[42−44] Bereznai et al. reported recently that PLD using a Mo metal target under controlled N_2 pressure gave γ-Mo_2N films ($T_s = 523$ K).[44] An exception was the formation of β-$Mo_{16}N_7$ by ion beam assisted deposition on Si reported by Mudholka and Thompson.[49] They observed a (400) X-ray diffraction peak for the thin film and assigned the phase to β-$Mo_{16}N_7$. β-$Mo_{16}N_7$ was reported to be discernible from β-Mo_2N only by the presence of very weak peaks (at very high 2θ) due to its superstructure.[50] It is probable that the phenomena reported by Mudholka and Thompson are similar to the β-Mo_2N formation on Si in this study. Laser ablation in this study gave well-crystallized β-Mo_2N, suggesting the advantage of laser ablation combined with nitrogen radical irradiation as a synthetic method of well-crystallized nitrides.

The magnetic susceptibility and the electric resistance showed that β-Mo_2N phase prepared in this study was superconducting below 5.2 K. To our knowledge, there is no report that described explicitly the superconducting transition temperature of β-Mo_2N.

Conclusions

Pulsed laser deposition of a Mo metal target combined with nitrogen radical irradiation gave rise to well-crystallized β-Mo_2N nitride phase with a moderate orientation of (100) parallel to the Si substrate surface. The composition was $Mo_2N_{0.85}$. The β-Mo_2N film showed superconductivity below 5.2 K. Cell parameters of the crystalline phase in the oriented films were analyzed and were refined using multiaxes X-ray diffraction data, highlighting the film deposition experiments combined with multiaxes X-ray analysis as a useful methodology for metal nitride synthetic chemistry.

Acknowledgment. This work was partially supported by a COE project and a Grant-in-Aid from the Japan Ministry of Education for Science, Culture, Sports and Technology (MEXT) and a CREST project from the Japan Science and Technology Corporation (JST).

CM050708I

(48) Banik, G.; Ettmayer, P.; Vendl, A.; Kieffer, R. *High Temp.−High Pressures* **1979**, *11*, 349.

(49) Mudholka, M. S.; Thompson, L. T. *J. Appl. Phys.* **1995**, *77*, 5138−5143.

(50) Karam, R.; Ward, R. *Inorg. Chem.* **1970**, *9*, 1385−1387.

(51) Briggs, D., Seah, M. P., Eds. *Practical Surface Analysis*, 2nd ed.; Wiley: New York, 1990; Vol. 1, p 599.